Inventory of Supplemental Information

Figure S1. Micrographs of Nissl stained coronal sections through the medial septum show the location of septal cannulae in animals with place cell recordings. Related to Figure 1.

Figure S2. The reduction of theta power in hippocampus by septal inactivation is compared to the reduction of theta power in medial entorhinal cortex in a prior study (Brandon et al., 2011). Related to Figure 1.

Figure S3. The reduction of theta power is shown for each experiment and each animal. The panels include (A) the theta power reduction during each place cell recording and (B) the theta power reduction in simultaneous local field potential recordings from the hippocampus and the medial entorhinal cortex. Related to Figure 1.

Figure S4. Recordings from place cells in a familiar environment during inactivation of the medial septal area. Related to Figures 2 and 3.

Figure S5. The place field stability in a novel room is compared between muscimol and control infusions using 5-minute intervals instead of the 10-minute intervals shown in Figures 2 and 3. Related to Figures 2 and 3.

Table S1. Descriptive statistics of spiking properties of place cells across sessions in the septal inactivation and control conditions. Related to Figure 1.

Table S2. Kolmogorov-Smirnov statistic results for place cell stability comparisons. Related to Figures 2 and 3.

Supplemental Experimental Procedures

Supplemental References

Supplemental Figures and Legends

Figure S1, Related to Figure 1

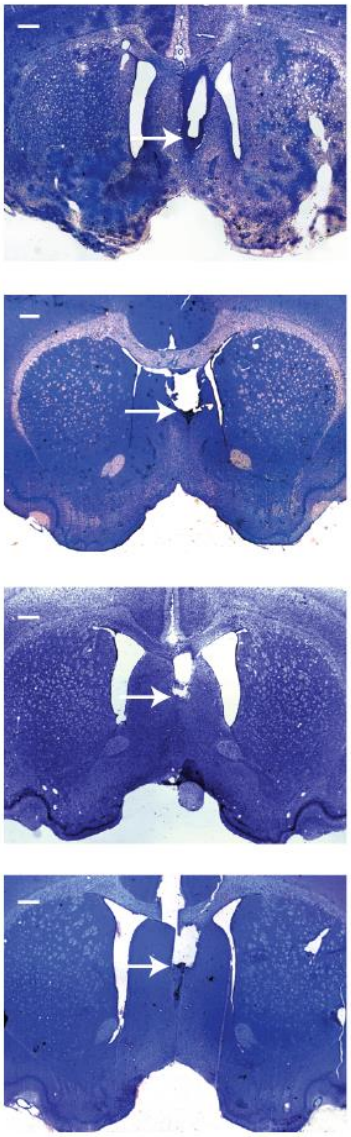

Figure S1. Septal cannula placements. Cresyl violet stains of coronal sections through the septal area. One image is shown for each experimental animal with place cell recordings (n animals = 4). These sections confirm that the drug infusion cannula (location of tip marked with white arrow) terminated within the septal area in all four animals. Scales bars, 0.5 mm.

Figure S2, Related to Figure 1

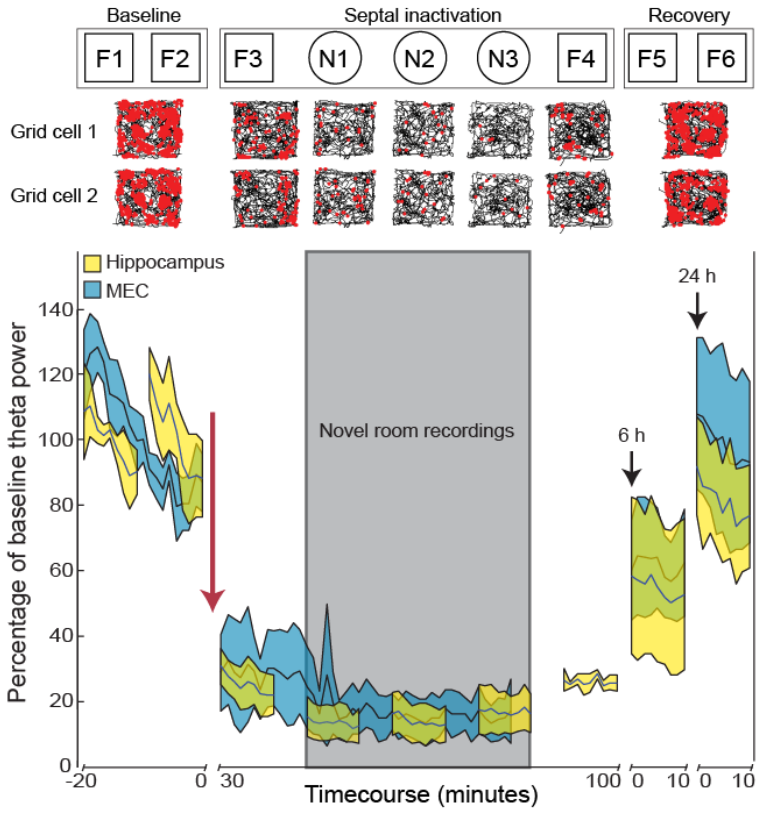

Figure S2. (Top) Experimental timeline of familiar (F) and novel (N) room recordings during baseline (F1, F2), septal inactivation (F3, N1, N2, N3, F4), and recovery from inactivation (F5, F6). Middle: Along with the MEC LFP recordings in three animals, two grid cells were recorded in one animal. As previously observed for all grid cells at these levels of theta reduction, the two cells that were recorded in this study also showed a clear disruption of spatial firing in the familiar and novel environment during septal inactivation. These data are consistent with the findings of Brandon et al. (2011) who also used intraseptral muscimol infusions and reported that 33 of 33 grid cells were disrupted. Below: Mean percentage of baseline theta (5-10 Hz) power after muscimol infusions into the septal area. The magnitude and timecourse of the reduction in theta power in hippocampus (mean ± 95% confidence intervals in yellow) was compared to the reduction of theta power in the medial entorhinal cortex (MEC, in blue) during the grid cell recordings in the dataset from Brandon et al. (2011). The timecourse of theta power reduction in our place cell recordings matched the timecourse of the theta reduction during the previously published grid cell recordings [n hippocampus = 5, n MEC = 10, between groups, $F(1, 416) = 0.006$, n.s.; interaction between time and group, $F(32,426) = 1.01$, n.s., two sample repeated measures ANOVA]. Furthermore, we confirmed that there was also a matching reduction in theta power when LFP was recorded simultaneously in the hippocampus and MEC (see Figures 1C, 1D, and S3).

Figure S3, Related to Figure 1

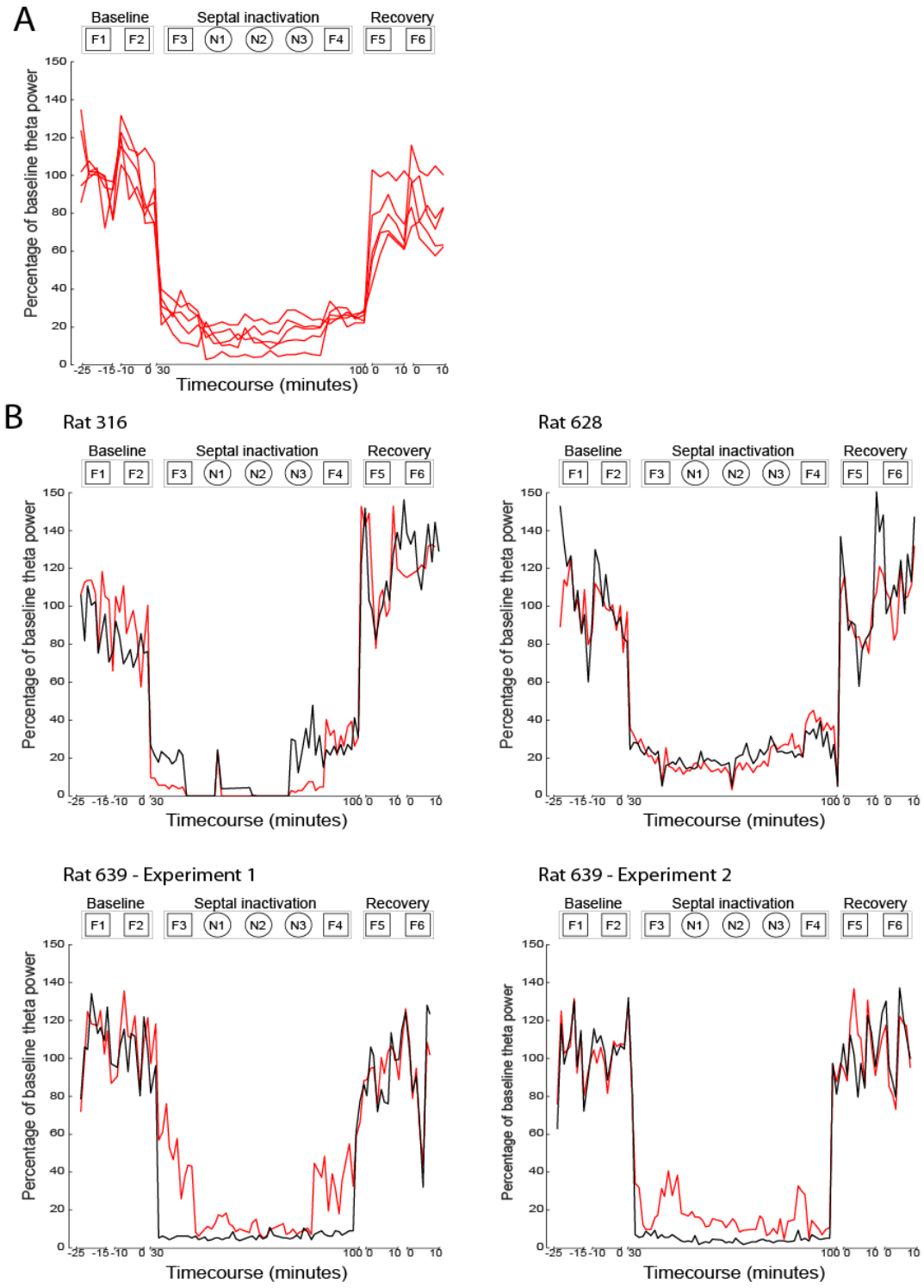

Figure S3. (A) Reduction of hippocampal theta power in each experiment with place cell recordings. Muscimol was infused into the medial septal area between F2 and F3, and the timecourse of the recordings in the familiar and in the novel room is as described in Figure S2. (B) Data from four additional experiments (from three animals) with simultaneous recordings of theta oscillations in the hippocampus and medial entorhinal cortex. Red lines correspond to theta power in the hippocampus and black lines correspond to theta power in the medial entorhinal cortex. The timecourse of theta reduction was parallel between medial entorhinal cortex and hippocampus during each experiment.

Figure S4, Related to Figure 2

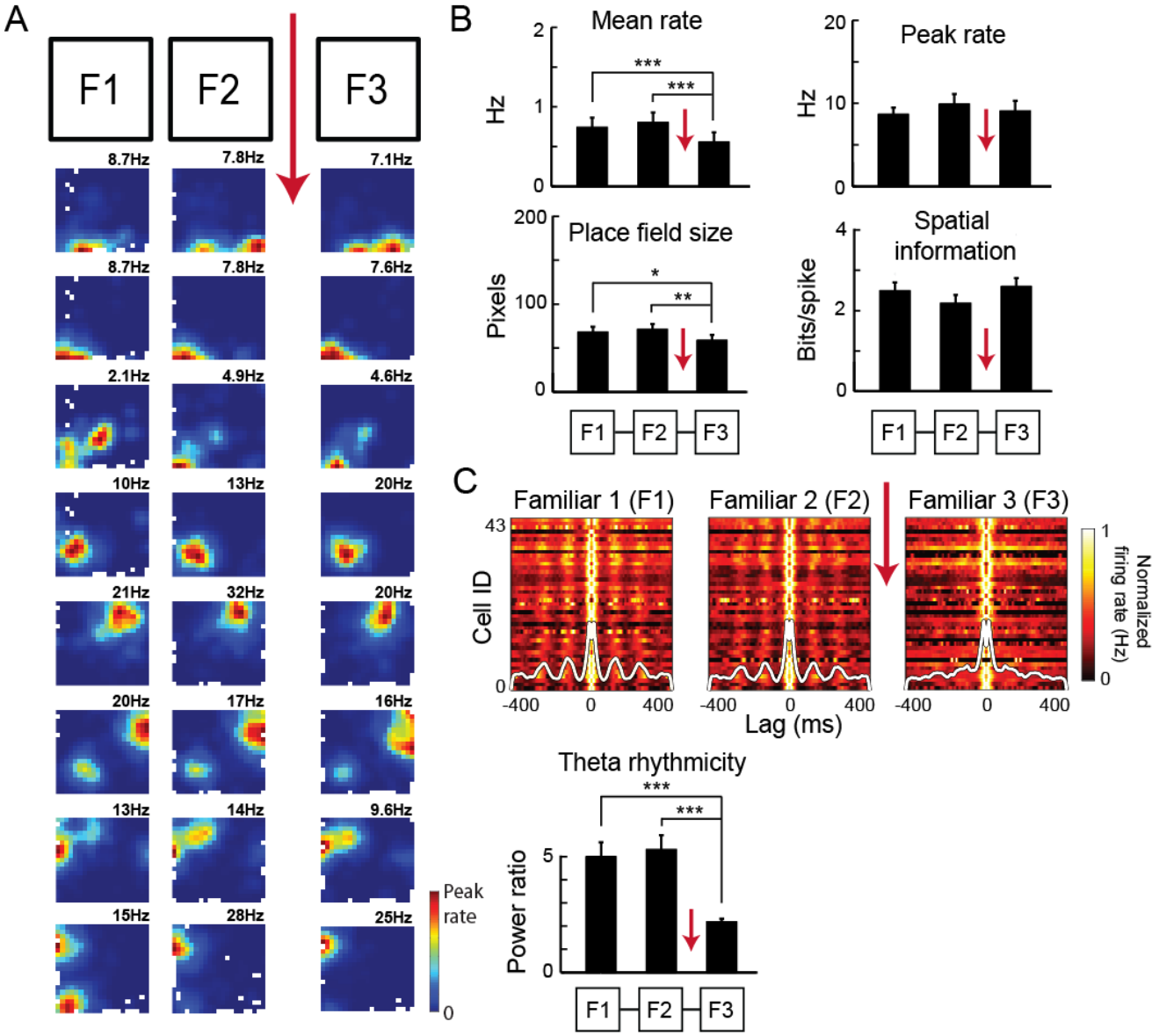

Figure S4. Place fields remained stable in a familiar room during muscimol inactivation of the medial septum. (A) Firing rate maps from hippocampal neurons recorded in a familiar room during baseline (F1 and F2) and septal inactivation (F3). Red arrow depicts when infusion of muscimol into the medial septal area occurred. Each row is a cell. (B) Bar graph displays mean and standard error of the mean (SEM) of spiking statistics during the baseline (F1, F2) and inactivation (F3) sessions. The mean firing rate and the size of place fields was reduced during the inactivation (mean rate, n = 65, F1:F3 and F2:F3, $P < 0.001$, place field size, n cells = 43, F1:F3, $P < 0.05$, F2:F3, $P < 0.001$) whereas the peak spatial firing rate and spatial information were unaffected by the inactivation (n cells = 43, all n.s.). These findings replicate the place field stability that was observed in a familiar environment with intraseptal lidocaine infusions Koenig et al. (2011) but muscimol has a lesser effect on the average firing rate. (C) Heat map of vertically stacked spike time autocorrelograms of all active cells in F1, F2, and F3 (n cells = 43). For each neuron (single rows), the zero-lag peak was removed and the autocorrelogram was normalized to its peak value. The averaged population autocorrelogram for each condition is overlaid in white. Below: Bar graph illustrates that theta rhythmicity was reduced during septal inactivation (n cells = 43, F1: F3 and F2: F3, $P < 0.001$).

Figure S5, Related to Figures 2 and 3

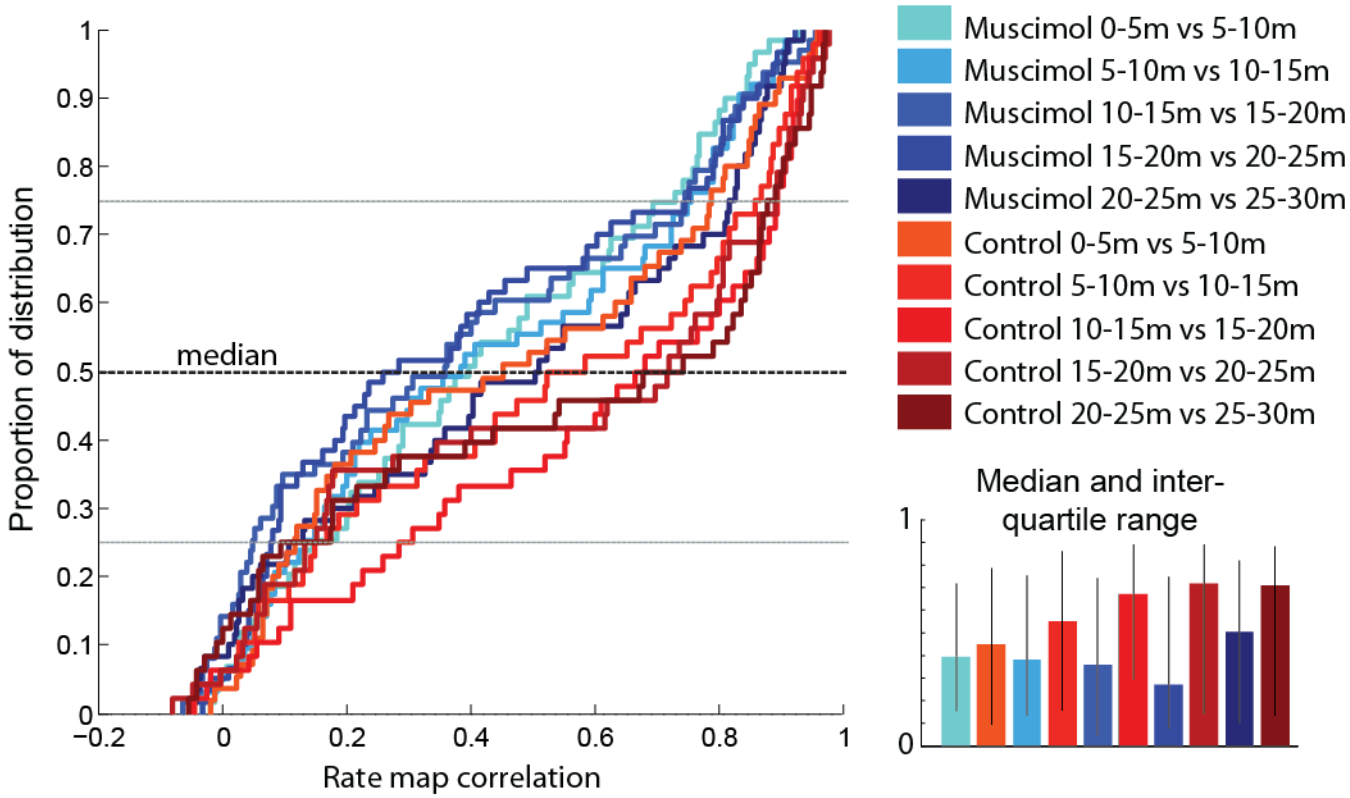

Figure S5. Place field stability in the novel room is compared between control and inactivation experiments. Place field stability was measured as the correlation between rate maps for each five minute interval. (Left) Cumulative density plots show the stability of place fields recorded after muscimol infusion (shades of blue) and after artificial cerbral spinal fluid (aCSF) infusion (shades of red). In the muscimol condition place field stability does not steadily increase with the amount of exposure to the novel room. In contrast, place fields recorded after infusion of aCSF into the medial septal area (control) showed a gradual increase in stability over time.

Supplemental Tables

Table S1

A Descriptive statistics for place cell spiking during muscimol condition

	F1	F2	F3	N1	N2	N3	F4	F5
Theta rhythmicity (power ratio)	4.75 ± 0.51	5.08 ± 0.67	1.89 ± 0.25	1.5 ± 0.24	1.64 ± 0.22	1.77 ± 0.35	2.44 ± 0.38	3.4 ± 0.39
Mean firing rate (Hz)	0.73 ± 0.11	0.76 ± 0.12	0.53 ± 0.1	0.8 ± 0.13	0.67 ± 0.13	0.75 ± 0.13	0.51 ± 0.09	0.55 ± 0.09
Peak rate (Hz)	10.23 ± 0.88	11.36 ± 1.17	10.67 ± 1.27	10.55 ± 1.16	10.18 ± 1.27	9.05 ± 0.85	10.36 ± 1.28	11.08 ± 1.40
Spatial information (bits/spike)	2.4 ± 0.26	2.13 ± 0.18	2.48 ± 0.25	2.18 ± 0.18	2.03 ± 0.18	2.28 ± 0.21	2.18 ± 0.17	2.35 ± 0.14
Place field size (pixels)	66.37 ± 5.62	69.77 ± 6.89	57.58 ± 5.69	81.26 ± 7.46	78.27±7.55	77.02 ± 8.39	59.47 ± 5.83	68.04 ± 6.14

B Descriptive statistics for place cell spiking during control condition

	F3	N1	N2	N3
Theta rhythmicity (power ratio)	4.80 ± 0.86	4.81 ± 0.6	5.20 ± 0.73	4.73 ± 0.61
Mean firing rate (Hz)	0.74 ± 0.15	1.61 ± 0.25	1.70 ± 0.25	1.47 ± 0.20
Peak rate (Hz)	8.97 ± 1.42	14.45 ± 1.76	14.50 ± 1.49	14.02 ± 1.41
Spatial information (bits/spike)	2.48 ± 0.33	1.62 ± 0.17	1.83 ± 0.16	2.19 ± 0.20
Place field size (pixels)	70.04 ± 10.60	130.85 ± 13.45	119.39 ± 11.9	101.03 ± 9.26

Table S1. Descriptive statistics for spiking properties of hippocampus neurons. (A) The mean and standard error of the mean (SEM) is reported for single-unit spiking properties including theta rhythmicity (power ratio), mean firing rate (Hz), peak rate (Hz), spatial information (bits/spike) and place field size for all sessions before (F1, F2), during (F3, N1, N2, N3, F4), and after (F5) inactivation of the medial septum. (B) Spiking statistics after control infusions of aCSF (F3, N1, N2, N3).

Table S2

Familiar vs Familiar		KS Stat	P value
F1:F2	F1:F3	0.194	n.s.
F1:F2	F3:F4	0.2126	n.s.
F1:F3	F3:F4	0.1154	n.s.
Familiar vs Novel			
F1:F2	N1:N2	0.3474	< 0.001
F1:F2	N1:N3	0.4651	< 0.001
F1:F2	N2:N3	0.3867	< 0.001
F3:F4	N1:N2	0.2028	n.s.
F3:F4	N1:N3	0.2879	< 0.01
F3:F4	N2:N3	0.2279	< 0.05
aCSF vs Muscimol in New Room			
N1:N2	N1:N2	0.1844	n.s.
N1:N3	N1:N3	0.112	n.s.
N2:N3	N2:N3	0.2873	< 0.05

Table S2. Summary statistics of place field stability in the familiar and new rooms. Results from two-sample Kolmogorov-Smirnov tests are reported for rate map stability between conditions including familiar versus familiar, familiar versus novel, and control (aCSF, artificial cerebral spinal fluid) versus septal inactivation in the new room.

Supplemental Experimental Procedures

Subjects and surgeries. Six male Long-Evans rats (3-6 month old, 425-550 g) were subjects in this study. Animals were housed individually in Plexiglas cages, maintained on a reverse 12-h light/12-h dark cycle at ~90 % of ad libitum weight, and given free access to water. All behavioral experiments were conducted during the dark phase of the light cycle. Prior to surgery, animals were habituated to handling by the experimenters and were trained to forage in an open field environment that would later serve as the 'familiar' recording arena.

Animals were implanted with a multi-electrode drive ('hyperdrive') aimed at the hippocampus and/or the entorhinal cortex and a drug infusion cannula aimed at the medial septal area. Anesthesia was induced with 3 % vaporized isoflurane in oxygen, and buprenorphine (0.02 mg/kg) was then administered for analgesia. Animals were continuously monitored for the level of anesthesia and were maintained at 1.5-2.0 % isoflurane for the duration of surgery. Two anchor screws, positioned anterior to bregma, were used as a recording ground. The septal infusion guide cannula (24-gauge) was preloaded with an internal dummy cannula, and was secured with dental acrylic to terminate just above the medial septum [anterior/posterior (AP): +0.06 mm, medial/lateral (ML): -1.1 mm, dorsal/ventral (DV): 4.3 mm; angled 10 degrees medially]. To implant hyperdrives (described below), a craniotomy was performed directly above the right hippocampus and/or above the entorhinal cortex, and the dura was removed. The hyperdrive was lowered such that the bottom of the drive bundle made contact with the dorsal surface of the brain. Kwik-sil or Neuroseal was applied to the remaining brain surface, and the hyperdrive was secured to the skull with a thick layer of dental acrylic. Tetrodes were lowered ~1 mm below the dorsal surface at surgery. Three animals were implanted with a hyperdrive aimed at the hippocampus (AP: -4.0 mm, ML: -3.0 mm). One animal was implanted with a split hyperdrive aimed at the hippocampus (AP: -4.3 mm, ML: -3.0 mm) and medial entorhinal cortex (MEC) (AP: 0.5 mm anterior to the transverse sinus, ML -4.6, angled 30 degrees

posteriorly) for simultaneous field potential recordings, and two animals were implanted with a hyperdrive aimed at the MEC (AP: most posterior tetrodes just anterior to the transverse sinus, ML -4.6) and an electrode aimed at the hippocampal fissure (AP: -4.0 mm, ML: -3.0 mm, DV: -2.5 mm). Animals were sutured if necessary and were returned to their home cage for monitoring. Animals were allowed five days of recovery prior to further behavioral testing.

Neurophysiology equipment and recordings. Single-units were recorded using the chronically implanted hyperdrive, which contained 12 recording tetrodes (bundles of four 17 micron platinum-iridium (90/10%) wires) and two reference tetrodes. All tetrodes could be individually moved along the dorso-ventral axis. Recording tetrodes were targeted to the CA1 pyramidal layer or to the dorsal MEC. A preamplifier (unity-gain operational amplifier located on the head stage), tether, and a motorized commutator connected the hyperdrive to a 64-channel digital data acquisition system (Neuralynx, Inc.). Signals were amplified (5,000-20,000x) and bandpass filtered (600-6,000 Hz) to isolate spiking events. Spike waveforms above a trigger threshold (25-55 µV) were time-stamped and digitized at 32 kHz for 1 ms. Local field potential (LFP) signals were sampled from the tetrodes and from the additional electrodes at 2,000 Hz and were amplified (5,000-20,000x) and band-pass filtered (0.1-9,000 Hz; Neuralynx, Bozeman, MT). Identical acquisition systems and recording settings were used in the familiar and in a new room during each series of recordings.

Intracranial microinfusions. Muscimol, a $GABA_A$ agonist, was diluted in sterile artificial cerebral spinal fluid (aCSF) (0.5 µg muscimol/µl aCSF). Prior to the infusion, the dummy cannula was removed to allow access to the guide cannula. An injector cannula (33-gauge), cut to a length 1 mm longer than the guide cannula, was filled with the diluted muscimol and lowered through the guide cannula into the medial

septum. A microinfusion pump infused 0.50 microliters of diluted muscimol at 0.25 µl/min. The injector cannula remained connected for two minutes after the infusion. The injector was then removed and a sterilized dummy cannula was reinserted and secured inside the guide cannula. To allow for diffusion of the drug, a 30-min delay period was imposed prior to further recordings. LFP was recorded after the 30-min period, and muscimol infusions that did not cause a visually apparent reduction in theta oscillations were considered failed infusion attempts and data acquisition ceased (n = 1). Control experiments were conducted in two of the four animals in this study. Here, all procedures were identical except that aCSF instead of muscimol was infused into the septal area. Because the lack of theta reduction was readily apparent while monitoring the recordings, experimenters were not blind to whether the infusion contained muscimol or aCSF.

Experimental timecourse. The experimental timecourse was designed to examine neural activity in a familiar and novel environment during septal inactivation. For this, we used the observation that the GABA-A agonist muscimol is long-acting and known to silence neural activity for 3-5 h. This time course permitted recordings in multiple recording sessions in the novel room while the septum remained inactive and we could test whether the firing of hippocampal cells changed during repeated 10-min sessions in the environment that was initially novel.

Prior to surgery, animals were trained daily for one week to forage for food reward (Cheerio crumbs) in a single room that became the ‘familiar’ environment for all experiments. The familiar environment consisted of a black-walled square (80 x 80 cm or 120 x 120 cm) which was centered in a cue-rich room and which contained a white vertical cue card on one wall to serve as an orienting landmark. Following recovery from surgery, animals were trained daily in the familiar room for a minimum of 11 days (two

times 10 min per day), and tetrode tips were gradually positioned in the CA1 pyramidal cell layer or in dorsal MEC during this period. Three other recording rooms in the laboratory were available as novel rooms and contained a circle (16-sided gray polygon, radius of 50 cm) or square (80 x 80 cm) novel recording environment. Importantly, animals never entered these novel rooms until after the medial septum was inactivated.

All recording sessions were 10 min in duration with 5-min intersession intervals except after the muscimol infusion when the interval was 30 min. CA1 recordings were conducted over a series of experimental conditions including: two baseline sessions in the familiar room (F1, F2), one session in the familiar room (F3), three sessions in a room that was initially novel (N1, N2, N3), and then one session back in the familiar room (F4). A 'recovery' session was recorded in the familiar room six hours after the infusion (F5), at a time when the drug effect had worn off. Only cells which could be reliably tracked over the entire recording sequence were included in the data analysis. In cases in which single-units appeared consistent over 24 hours, additional recordings were performed on the day after muscimol infusion. These recordings consisted of one session in the familiar room (F6), two sessions in the room that was novel on the previous day (N4, N5), and then a final session in the familiar room (F7). Only cells that could be reliably tracked from the previous day were included in the analysis.

Postmortem confirmation of recording locations. Tetrodes were not moved after the final recording session. Animals were overdosed with sodium pentobarbital and were perfused intracardially with PBS and then 4 % formaldehyde. Brains were extracted and were stored in 4 % formaldehyde at 6 °C for at least 24 hours. Approximately three days prior to slicing, brains were transferred into a 30 % sucrose solution for cryoprotection. A microtome was used to obtain coronal section through the medial septum and

hippocampus. Tissue was mounted on glass slides and stained with a cresyl violet stain. Hippocampal recording tetrodes that had well-isolated neurons were confirmed to terminate in or near the principal cell layer of region CA1 (**Figure 1B**).

Single unit identification. Methods for cluster cutting and cell tracking were the same as described previously (Brandon et al., 2011; Koenig et al., 2011; Mankin et al., 2012). Briefly, single-units were manually isolated 'offline' using a custom-modified version of MClust, a cluster cutting GUI for MATLAB (Redish, A.D. MClust. http://redishlabneuroscienceumnedu/MClust/MClusthtml). Neurons were separated based on the peak amplitude, peak-to-valley amplitude, and energy of spike waveforms. Evaluation of the presence of biologically realistic inter-spike intervals, temporal autocorrelations, and cross correlations was used to confirm single-unit isolation. Neurons that were not separable in cluster space were removed from the analysis. For inactivation experiments, waveform profiles across the four electrodes and cluster position were compared across recordings sessions to confirm the stability of each neuron.

Position estimation. To track the position of the animal during each recording session, a ceiling-mounted video camera detected an array of light emitting diodes (LEDs) mounted on the recording head stage just above the head of the animal. The position of the LEDs was sampled at 30 Hz and the rat's x-y coordinate was calculated as the centroid of the LED array. Up to five consecutive missing samples, due to occlusion of the LEDs or reflections in the environment, were replaced by linear interpolation of position before and after the lost samples.

Theta power of local field potentials. LFPs obtained from the hippocampus and MEC were referenced to a cortical reference tetrode that did not show evidence of theta oscillations when referenced to ground. For

each experiment, LFP from the tetrode with the highest mean power between 5-10 Hz in the first baseline session (F1) was selected for analysis. Throughout each recording, we calculated the mean power within 1 Hz of the theta peak of the power spectra during 2-min sliding windows to compare the relative theta power before, during, and after inactivation of the septal area. Power spectra were smoothed by a convolution with a Gaussian kernel (standard deviation of 0.2 Hz). The power in each window was divided by the average of all windows during the baseline conditions to determine the percentage of baseline theta power.

Spike train rhythmicity. Theta rhythmicity of spike trains was quantified by calculating the temporal autocorrelation of the spike train using an unbiased normalization by the number of bins (bin width = 8 ms) at each lag. The center peak (0 ms lag) was removed. A theta power ratio was calculated to determine the degree of theta power in the spike time autocorrelation, as the ratio of the mean power within 1 Hz of the highest peak in the power spectrum between 7 and 11 Hz to the mean signal power between 0-15 Hz. For visualization, firing rate normalized autocorrelations were color-coded with a black to bright orange color scale corresponding to normalized values between 0 and 1 (Figs. 2C and S4C). The averaged population autocorrelation for each condition was calculated by averaging the autocorrelation at each lag for all cells in the condition.

Spatial tuning and spatial correlation. Firing rate maps of cell spiking in the open field were constructed by calculating the occupancy normalized spike count for 4 cm x 4 cm bins of position data. Data were smoothed by a two-dimensional convolution with a pseudo-Gaussian kernel with a standard deviation of one pixel (4 cm). Rate map correlations were computed from the smoothed rate maps to determine the similarity between spatial firing between conditions. For each correlation, we calculated Pearson's linear

correlation coefficient for all pixels that had non-zero occupancy in both rate maps. Spatial information (bits/spike) for each cell in each condition was calculated from the smoothed rate maps, as,

$$I = \sum p_i \cdot \frac{F_i}{F} \cdot \log\left(\frac{F_i}{F}\right)$$

where I is the spatial information in bits/spike, p_i is the probability of occupancy in pixel i, F_i is the mean firing rate for pixel i, and F is the mean firing rate. The peak spatial firing rate was defined as the firing rate of the pixel that contained the highest firing rate. Place field size was calculated for each cell with a minimum peak rate of 5 Hz as the number of adjacent pixels that contained equal to or greater than 20% of the firing rate of the pixel with the highest firing rate. Multiple fields were included if each field consisted of at least 5 pixels.

Statistical Analysis. All statistical comparisons were calculated using MATLAB r2009b. In particular, Wilcoxon's paired, two-sided sign rank test (signrank, MATLAB) was used when comparing spatial firing properties across repeated exposures to same room (familiar or novel), and the Wilcoxon's two-sided rank sum test (ranksum, MATLAB) was used when comparing spatial properties between place cell populations that were active in the muscimol and control infusions. A two-sample Kolmogorov-Smirnov test was used to compare cumulative distribution functions for firing rate overlap and firing rate map correlation comparisons. These tests do not assume normality. For comparisons of the reduction in theta power, we used a two-sample repeated measure ANOVA.

Supplemental References

Mankin, E.A., Sparks, F.T., Slayyeh, B., Sutherland, R.J., Leutgeb, S., and Leutgeb, J.K. (2012). Neuronal code for extended time in the hippocampus. Proc Natl Acad Sci U S A *109*, 19462-19467.